

On the Purity of the ZZ Ceti Instability Strip: Discovery of More Pulsating DA White Dwarfs on the Basis of Optical Spectroscopy¹

P. Bergeron and G. Fontaine

*Département de Physique, Université de Montréal, C.P. 6128, Succ. Centre-Ville,
Montréal, Québec, Canada, H3C 3J7.*

bergeron@astro.umontreal.ca, fontaine@astro.umontreal.ca

M. Billères

*European Southern Observatory, Santiago Headquarters, Avenida Alonso de Cordova 3107,
Vitacura, Casilla 19001, Santiago 19, Chile.*

mbilleres@eso.org

S. Boudreault

*Département de Physique, Université de Montréal, C.P. 6128, Succ. Centre-Ville,
Montréal, Québec, Canada, H3C 3J7.*

boudreault@astro.umontreal.ca

and

E.M. Green

Steward Observatory, University of Arizona, Tucson, AZ 85721.

egreen@as.arizona.edu

ABSTRACT

We report the discovery of two new ZZ Ceti pulsators, LP 133–144 and HE 1258+0123, selected on the basis of model atmosphere fits to optical spectroscopic data. The atmospheric parameters for LP 133–144, $T_{\text{eff}} = 11,800 \pm 200$ K and $\log g = 7.87 \pm 0.05$, and for HE 1258+0123, $T_{\text{eff}} = 11,410 \pm 200$ K and $\log g = 8.04 \pm 0.05$, place them within the empirical boundaries of the ZZ Ceti instability strip. This brings the number of known ZZ Ceti stars to a total of 36, a quarter of which have now been discovered using the spectroscopic approach for estimating their atmospheric parameters. This method has had a 100% success

rate so far in predicting the variability of candidate ZZ Ceti stars. We have also analyzed additional spectra of known nonvariable white dwarfs in the vicinity of the ZZ Ceti instability strip. Our study further strengthens the idea that ZZ Ceti stars occupy a pure region in the $\log g - T_{\text{eff}}$ plane, a region where no nonvariable stars are found. This result supports the thesis that ZZ Ceti pulsators represent a phase through which *all* DA stars must evolve.

Subject headings: stars: fundamental parameters — stars: individual (LP 133–144, HE 1258+0123) — stars: oscillations — white dwarfs

1. Introduction

Pulsating hydrogen line (DA) white dwarfs — or ZZ Ceti stars — are found in a rather narrow range of effective temperature, between about $T_{\text{eff}} = 12,500$ K and 11,100 K according to the detailed study of Bergeron et al. (1995, hereafter B95), with the temperatures defining the blue and red edges depending on the mass of the white dwarf. Asteroseismological studies of these stars provide important constraints on their internal structure, including their chemical layering. If ZZ Ceti stars truly represent an evolutionary phase through which *all* DA white dwarfs must go through, then the results obtained for the pulsators can be generalized to the entire class of DA stars as well. In particular, the asteroseismological determinations of the hydrogen and helium envelope masses in DA white dwarfs can be used as “calibration” of these quantities in cooling calculations. Hence it is important to determine the fraction of white dwarfs inside the ZZ Ceti instability strip that are nonvariable. More than twenty years ago, Fontaine et al. (1982) have argued from a study of multichannel photometric data that the strip is most likely pure. This question of the purity of the ZZ Ceti instability strip has been debated in the meantime by various authors (e.g., Dolez et al. 1991; Kepler & Nelan 1993; Kepler et al. 1995; Silvotti et al. 1997; Giovannini et al. 1998) who claimed, contrary to Fontaine et al. (1982), that the strip contains both variable and nonvariable stars. A definite answer to this question had to wait for a more precise method of measuring the atmospheric parameters of ZZ Ceti stars and other white dwarfs in the vicinity of the instability strip.

B95 have developed such a theoretical framework for measuring the effective temperature and surface gravity of ZZ Ceti stars by comparing high signal-to-noise ratio ($S/N \gtrsim 80$)

¹Based, in part, on observations gathered at the European Southern Observatory, La Silla, Chile.

spectroscopic observations with the predictions of model atmospheres. The method uses simultaneous fits to the Balmer lines, from H β to H9. This so-called spectroscopic technique has first been applied to hotter white dwarfs by Bergeron et al. (1992) to determine the mass distribution of DA stars, and it is arguably the most precise method for measuring the atmospheric parameters of white dwarf stars. Although the approach used by B95 has been the subject of various criticisms, Fontaine et al. (2003) have reviewed and rebutted all the arguments that have been put forward against the use of optical spectroscopy. In particular, Fontaine et al. (2003) have demonstrated the usefulness of the spectroscopic technique to obtain accurate measurements of the atmospheric parameters of ZZ Ceti stars as well as neighboring stars in the $\log g - T_{\text{eff}}$ diagram, and to predict the variability of ZZ Ceti candidates. Fontaine et al. have also shown that the atmospheric parameters for all 34 known ZZ Ceti stars and 103 nonvariable stars obtained with the optical spectroscopy approach define a very narrow region in the $\log g - T_{\text{eff}}$ plane in which *no* nonvariable stars are found (see Fig. 3 of Fontaine et al. 2003), in agreement with our thesis that ZZ Ceti stars represent a phase through which all DA white dwarfs must evolve.

With this powerful diagnostic tool in hand, it becomes possible to identify ZZ Ceti candidates from large white dwarf samples by securing spectroscopic observations for all objects, and by determining T_{eff} and $\log g$ values from model atmosphere fits to optical spectroscopy. To obtain reliable and consistent results, however, three conditions must be met: (1) High-quality spectra must be gathered, (2) model atmospheres comparable to those of B95 (and based on the calibration of the mixing-length theory proposed there) must be used, and (3) attention to details must be provided (see B95 and references therein). Stars with atmospheric parameters overlapping the currently known ZZ Ceti stars ought to be variable according to our past results. There are currently 34 known ZZ Ceti stars, 7 of which have been discovered using the spectroscopic technique: GD 165 (Bergeron & McGraw 1990), HS 0507+0435B (Jordan et al. 1998), PG 1541+650 (Vauclair et al. 2000), GD 244 and KUV 02464+3239 (Fontaine et al. 2001), and more recently MCT 0145–2211 and HE 0532–5605 (Fontaine et al. 2003). In this paper we present spectroscopic fits that led to the discovery of two more pulsators, LP 133–144 and HE 1258+0123, for a total of 36 ZZ Ceti stars known up to date. We also present an upgraded view of the ZZ Ceti instability strip in the $\log g - T_{\text{eff}}$ diagram.

2. LP 133–144

Liebert et al. (2003) have recently obtained high S/N spectroscopy of all DA white dwarfs identified in the Palomar-Green (PG) survey (Green et al. 1986). One of the goals

of that effort is to derive an improved luminosity function using the spectroscopic approach. Among the 347 DA stars analyzed in that way, 9 objects were previously known to be ZZ Ceti variables (GD 99, G117–B15A, GD 154, G238–53, GD 165, PG 1541+651, R808, PG 2303+243, and G29–38). Among the remaining PG stars, only one object, LP 133–144 (PG 1349+552, WD 1349+552, $B_{\text{ph}} \simeq 16.0$), has atmospheric parameters ($T_{\text{eff}} = 11,800$ K and $\log g = 7.87$) consistent with it being a ZZ Ceti pulsator. Our best fit using $\text{ML2}/\alpha = 0.6$ models (see B95) is shown in Figure 1.

Because Balmer lines in the ZZ Ceti range are, in fact, very sensitive to both T_{eff} and $\log g$, internal errors obtained from least-squares fits to high S/N optical spectra are meaningless, as discussed in detail by Bergeron et al. (1992) and B95. The typical good fits that are achieved only reflect the ability of the model spectra to match the data, and the error budget is actually dominated by uncertainties of the flux calibration. To estimate the true external errors, Fontaine et al. (2003) have compared the atmospheric parameters of a subset of ZZ Ceti stars taken from B95 with those derived from independent spectra obtained by Chris Moran (2000, private communication), using a completely different setup and reduction procedure (see also Bergeron et al. 1992, for a similar comparison at higher temperatures). As can be seen from Figure 2 of Fontaine et al. (2003), the standard deviations between both sets of measurements allow us to estimate the real external errors for stars in the ZZ Ceti range, $\sigma(T_{\text{eff}}) \sim 200$ K and $\sigma(\log g) \sim 0.05$. Since all the stars in this paper are found in the same temperature range (see Fig. 1 of Fontaine et al. 2003) and have been observed with the same setup and signal-to-noise ratio, we adopt these uncertainties throughout.

To our knowledge, LP 133–144 had never been observed before for photometric variability, most likely because there is no published color information on this white dwarf (see Fontaine et al. 2001 for a historical account of the selection criteria used previously for uncovering ZZ Ceti stars). As part of an ongoing program to identify new ZZ Ceti pulsators, we observed LP 133–144 in integrated (white light) “fast” photometric mode at the Steward Observatory Mount Bigelow Station 1.6 m telescope during four nights in March-April 2003. The photometric observations were obtained with LAPOUNE, the portable Montréal three-channel photometer. A total of 17.6 h of data was gathered. The top two panels of Figure 2 show our sky-subtracted, extinction-corrected light curves obtained during the discovery run. Clearly, LP 133–144 is a multiperiodic luminosity variable, a new ZZ Ceti star.

The top panel of Figure 3 shows the resulting Fourier (amplitude) spectrum of the light curve of LP 133–144 using all the 17.6 h of data. From this spectrum, we can easily identify four main frequency components corresponding to periods in the range from 209.2 to 327.3 s. We note that the relatively short periods and low amplitudes ($\lesssim 1\%$) of the luminosity variations detected in LP 133–144 are consistent with its location near the blue edge of the

ZZ Ceti instability strip (see § 4).

3. HE 1258+0123

The two ZZ Ceti stars MCT 0145–2211 and HE 0532–5605 recently discovered by Fontaine et al. (2003) have published T_{eff} and $\log g$ values taken from Koester et al. (2001) as part of the SPY program. These two ZZ Ceti candidates have been selected by Fontaine et al. because they happen to fall precisely in the middle of the empirical ZZ Ceti instability strip determined by B95. Two other SPY objects shown in Figure 3 of Fontaine et al. (2003), EC 12043–1337 (WD 1204–136, $V = 15.52$) and HE 1258+0123 (WD 1258+013, $V = 16.26$), fall also inside the instability strip, but very close to the cool edge of the strip. During our March-April 2003 observing run when the variability of LP 133–144 was discovered, we also obtained high speed photometric data on EC 12043–1337, which showed a constant light curve at the 2–3 millimag level. We had also secured similar observations on HE 1258+0123, but we later discovered that we had observed the wrong star, since the coordinates provided in Koester et al. (2001) for this object, $\alpha(2000) = 13:00:59.2$ and $\delta(2000) = +00:57:12$, correspond to the sdO star HE 1258+0113 according to Christlieb et al. (2001), who gives instead for HE 1258+0123 $\alpha(2000) = 13:01:10.5$ and $\delta(2000) = +01:07:39$.

In June 2003, we secured our own spectroscopic observations for both EC 12043–1337 and HE 1258+0123 using the 2.3 m telescope at the Steward Observatory Kitt Peak Station, equipped with the Boller & Chivens spectrograph and a Texas Instrument CCD detector. The spectral coverage is about $\lambda\lambda 3100$ –5300, thus covering H β up to H9 at an intermediate resolution of ~ 6 Å FWHM. Our best fit for EC 12043–1337 using our own model grid is shown in Figure 1. The atmospheric parameters for this object, $T_{\text{eff}} = 11,200$ K and $\log g = 8.23$, now place it close to, but below, the empirical red edge of the instability strip, in agreement with our high speed photometric result. Koester et al. (2001) obtained $T_{\text{eff}} = 11,111$ K and $\log g = 8.05$ for the same star.

Our spectroscopic solution for HE 1258+0123, $T_{\text{eff}} = 11,410$ K and $\log g = 8.04$, is shown in Figure 1, which can be compared with the results of Koester et al. (2001) for the same star, $T_{\text{eff}} = 11,161$ K and $\log g = 7.92$. These revised parameters push HE 1258+0123 even deeper within the empirical instability strip. On the basis of our previous success at predicting the variability of ZZ Ceti candidates using the optical spectroscopy approach, we figured that this star ought to be variable. One week later, one of us (M. B.) managed to obtain high speed photometric observations of HE 1258+0123 using the EMMI instrument attached to the 3.6 m New Technology Telescope (NTT) at the ESO La Silla Station. The exposure time was adjusted from 20 s to 15 s as the seeing improved, with corresponding

sampling times of 55 s and 49 s, respectively. Images were bias subtracted, flat fielded, and magnitudes were calculated using the mag/circ function of the MIDAS package. The 3.3 hour long photometric light curve is shown in the lower panel of Figure 2. The results confirm our expectation that HE 1258+0123 is indeed a multiperiodic luminosity variable, another ZZ Ceti star. The Fourier spectrum for this single run is displayed in the lower panel of Figure 3. The dominant peak at 744.6 s is consistent with this ZZ Ceti star being closer to the red edge of the instability strip than LP 133–144 (see § 4). Other important peaks are also present at 439.2, 528.5, and 1091.1 s. The sharp rises and slow declines observed in the light curve are characteristic of large amplitude ZZ Ceti stars.

4. The Empirical ZZ Ceti instability strip

Of the four SPY objects originally found inside the empirical instability strip (see Figure 3 of Fontaine et al. 2003), three remain within the strip according to our own spectroscopic analysis, and they correspond indeed to new ZZ Ceti stars (MCT 0145–2211, HE 0532–5605, and HE 1258+0123). For its part, the nonvariable white dwarf EC 12043–1337 has a revised effective temperature and a surface gravity that put it slightly below the empirical red edge of the strip. Two additional objects lie formally within, but very close to the *blue* edge of the instability strip shown in Figure 3 of Fontaine et al. (2003). The one at the top is LP 550–52 with $T_{\text{eff}} = 11,550$ K and $\log g = 7.65$, an unresolved degenerate binary with a period of 1.157 days according to Maxted et al. (1999). The atmospheric parameters for this object are thus an average of the parameters of both components of the system (Liebert et al. 1991), and we will no longer consider it in our analysis. The other object seen in Figure 3 of Fontaine et al. (2003) is GD 133 at $T_{\text{eff}} = 12,090$ K and $\log g = 8.06$. Given the uncertainties, the position of that object inside the strip, but very close to the blue edge, certainly remains consistent with the idea of a pure strip. Nevertheless, given that the spectrum we used for GD 133 had not been obtained by us, we reobserved it in June 2003 with our standard setup. Our revised atmospheric parameters, $T_{\text{eff}} = 12,290$ K and $\log g = 8.04$, now place GD 133 above the blue edge of the ZZ Ceti instability strip.

Our updated empirical ZZ Ceti instability strip is shown in Figure 4 where the positions of all known variables are indicated, together with the results for 54 known nonvariable white dwarfs. For the convenience of the reader, we provide in Table 1 a summary of the atmospheric parameters for all 36 known ZZ Ceti stars. The table assembles values taken from B95 (22 stars), Fontaine et al. (2003, 12 stars), and this paper (2 stars). The values of T_{eff} and $\log g$ are determined from $\text{ML2}/\alpha = 0.6$ models, while the stellar masses are derived from the models of Wood (1995) for carbon-core compositions, helium layers of

$M_{\text{He}} = 10^{-2}M_{\star}$, and hydrogen layers of $M_{\text{H}} = 10^{-4}M_{\star}$. Note that some very small changes appear with respect to some of the B95 data, the result of redoing the fits in a completely homogeneous way. The picture of the empirical instability strip that emerges from our results is that of a pure strip in which no nonvariable stars are found, a conclusion that supports our claim that ZZ Ceti stars represent a phase through which *all* DA stars must evolve. It has a trapezoidal shape in the $\log g - T_{\text{eff}}$ plane, with the blue edge showing a stronger dependence on the surface gravity than the red edge does, although this conclusion rests heavily on the most massive ZZ Ceti star in this diagram, LTT 4816 (WD 1236–495). The newly discovered ZZ Ceti stars reported in this paper are shown as bold open circles in Figure 4, and their location within the instability strip together with their dominant periods found from the Fourier spectra (Fig. 3) are consistent with the period-effective temperature relation observed in ZZ Ceti pulsators (see, e.g., Winget & Fontaine 1982).

In Figure 4 there appears to be a paucity of stars directly above the blue edge and below the red edge of the instability strip. However, our combined sample of variables and nonvariables is heavily biased against the latter since we have gathered spectra for only a fraction of them. Progress is underway to secure spectroscopic observations for all stars outside the boundaries of the instability strip, and to increase the number of nonvariable white dwarfs in the vicinity of the strip to help define better the exact location and shape of the red and blue edges.

The spectroscopic approach, when properly handled, provides the most powerful way for discovering new ZZ Ceti stars in a routine fashion, and it could be easily applied to large surveys such as the Sloan Digitized Sky Survey. Interestingly enough, HE 1258+0123 is also part of the Sloan survey (SDSS J 130110.51+010739.9) and its variability should be rediscovered as part of that ongoing survey.

We wish to thank the Director and staff of Steward Observatory for allowing us to use their facilities. This work was supported in part by the NSERC Canada and by the Fund NATEQ (Québec). G.F. also acknowledges the contribution of the Canada Research Chair Program.

REFERENCES

Bergeron, P., & McGraw, J. T. 1990, ApJ, 352, L45

Bergeron, P., Saffer, R. A., & Liebert, J. 1992, ApJ, 394, 228

Bergeron, P., Wesemael, F., Lamontagne, R., Fontaine, G., Saffer, R. A., & Allard, N. F. 1995, ApJ, 449, 258 (B95)

Christlieb, N., Wisotzki, L., Reimers, D., Homeir, D., Koester, D., & Heber, U. 2001, A&A, 366, 898

Dolez, N., Vauclair, G., & Koester, D. 1991, in White Dwarfs, ed. G. Vauclair & E.M. Sion (Kluwer: Dordrecht), 361

Fontaine, G., Bergeron, P., Billères, M., & Charpinet, S. 2003, ApJ, 591, 1184

Fontaine, G., Bergeron, P., Brassard, P., Billères, M., & Charpinet, S. 2001, ApJ, 557, 792

Fontaine, G., McGraw, J. T., Dearborn, D. S. P., Gustafson, J., & Lacombe, P. 1982, ApJ, 258, 651

Giovannini, O., Kepler, S. O., Kanaan, A., Costa, A. F. M., & Koester, D. 1998, A&A, 329, L13

Green, R. F., Schmidt, M., & Liebert, J. 1986, ApJS, 61, 305

Jordan, S., Koester, D., Vauclair, G., Dolez, N., Heber, U., Hagen, H.-J., Reimers, D., Chevreton, M., & Dreizler, S. 1998, A&A, 330, 277

Kepler, S.O., & Nelan, E.P. 1993, AJ, 105, 608

Kepler, S. O., Giovannini, O., Kanaan, A., Wood, M. A., & Claver, C.F. 1995, Baltic Astronomy, 4, 157

Koester, D., Napiwotzki, R., Christlieb, N., Drechsel, H., Hagen, H.-J., Heber, U., Homeier, D., Karl, C., Leibundgut, B., Moehler, S., Nelemans, G., Pauli, E.-M., Reimers, D., Renzini, A., & Yungelson, L. 2001, A&A, 378, 556

Liebert, J., Bergeron, P., Holberg, J. B., & Saffer, R. A. 2003, in preparation

Liebert, J., Bergeron, P., & Saffer, R. A. 1991, in White Dwarfs, ed. G. Vauclair & E.M. Sion (Kluwer: Dordrecht), 409

Maxted, P. F. L., & Marsh, T. R. 1999, MNRAS, 307, 122

Silvotti, R., Bartolini, C., Cosentino, G., Guarnieri, A., & Piccioni, A. 1997 in ASSL Conf. Ser. 214, 10th European Workshop on White Dwarfs, ed. J. Isern, M. Hernanz, & E. Garcia-Berro (Dordrecht: Kluwer), 489

Vauclair, G., Dolez, N., Fu, J. N., & Chevreton, M. 1997, A&A, 322, 155

Winget, D. E., & Fontaine, G. 1982, in Pulsations in Classical and Cataclysmic Variables, ed. J.P. Cox & C.J. Hansen (Boulder: Univ. of Colorado), 142

Wood, M. A. 1995, in 9th European Workshop on White Dwarfs, NATO ASI Series, ed. D. Koester & K. Werner (Berlin: Springer), 41

Table 1. Atmospheric Parameters of ZZ Ceti stars

WD	Name	T_{eff} (K)	$\log g$	M/M_{\odot}	M_V
0104–464	BPM 30551	11260	8.23	0.75	12.16
0133–116	R548	11990	7.97	0.59	11.63
0145–221	MCT 0145–2211	11550	8.14	0.69	11.97
0246+326	KUV 02464+3239	11290	8.08	0.65	11.93
0341–459	BPM 31594	11540	8.11	0.67	11.92
0416+272	HL Tau 76	11450	7.89	0.55	11.63
0417+361	G38–29	11180	7.91	0.55	11.71
0455+553	G191–16	11420	8.05	0.64	11.86
0507+045	HS 0507+0435B	11630	8.17	0.71	11.99
0517+307	GD 66	11980	8.05	0.64	11.75
0532–560	HE 0532–5605	11560	8.49	0.92	12.52
0836+404	KUV 08368+4026	11490	8.05	0.64	11.85
0858+363	GD 99	11820	8.08	0.66	11.83
0921+354	G117–B15A	11630	7.97	0.59	11.70
1137+423	KUV 11370+4222	11890	8.06	0.64	11.77
1159+803	G255–2	11440	8.17	0.71	12.04
1236–495	LTT 4816	11730	8.81	1.10	13.09
1258+013 ^a	HE 1258+0123	11410	8.04	0.63	11.84
1307+354	GD 154	11180	8.15	0.70	12.07
1349+552 ^a	LP 133–144	11800	7.87	0.53	11.53
1350+656	G238–53	11890	7.91	0.55	11.56
1401–147	EC 14012–1446	11900	8.16	0.70	11.92
1422+095	GD 165	11980	8.06	0.65	11.77
1425–811	L19–2	12100	8.21	0.74	11.96
1541+650	PG 1541+651	11600	8.10	0.67	11.90
1559+369	R808	11160	8.04	0.63	11.91
1647+591	G226–29	12460	8.28	0.79	12.02
1714–547	BPM 24754	11070	8.03	0.62	11.92
1855+338	G207–9	11950	8.35	0.83	12.22
1935+276	G185–32	12130	8.05	0.64	11.73

Table 1—Continued

WD	Name	T_{eff} (K)	$\log g$	M/M_{\odot}	M_V
1950+250	GD 385	11710	8.04	0.63	11.78
2254+126	GD 244	11680	8.08	0.65	11.84
2303+242	PG 2303+243	11480	8.09	0.66	11.90
2326+049	G29–38	11820	8.14	0.69	11.91
2347+128	G30–20	11070	7.95	0.58	11.80
2348–244	EC 23487–2424	11520	8.10	0.67	11.91

^aThis paper

Fig. 1.— Model fits to the individual Balmer line profiles of the new ZZ Ceti stars LP 133–144 and HE 1258+0123, and of the nonvariable white dwarf EC 12043–1337. The lines range from H β (bottom) to H9 (top), each offset vertically by a factor of 0.2. Values of T_{eff} and $\log g$ have been determined from $ML2/\alpha = 0.6$ models, while the stellar masses have been derived from the models of Wood (1995) for carbon-core compositions, helium layers of $M_{\text{He}} = 10^{-2} M_{\star}$, and hydrogen layers of $M_{\text{H}} = 10^{-4} M_{\star}$.

Fig. 2.— *Top two panels:* Light curve of LP 133–144, observed in “white light” with LA-POUNE attached to the Mount Bigelow 1.6 m telescope. Each point represents a sampling time of 10 s. *Bottom panel:* Light curve of HE 1258+0123 gathered using the EMMI instrument with no filter attached to the NTT. Each plotted point represents a sampling time of approximately 50 s. Both light curves are expressed in terms of residual amplitude relative to the mean brightness of the star.

Fig. 3.— Fourier (amplitude) spectra of the light curves of LP 133–144 and HE 1258+0123 in the 0–10 mHz bandpass. The spectra in the region from 10 mHz out to the Nyquist frequency are entirely consistent with noise and are not shown. The amplitude axis is expressed in terms of the percentage variations about the mean brightness of the star.

Fig. 4.— Surface gravity-effective temperature distribution for various samples of DA white dwarfs. The open circles represent the 36 known ZZ Ceti stars tabulated in Table 1; the bold open circles correspond to the newly identified ZZ Ceti stars LP 133–144 (*left*) and HE 1258+0123 (*right*). Filled circles are DA stars that are known to be nonvariable and whose atmospheric parameters have been determined by us on the basis of the same homogeneous approach as the ZZ Ceti stars. The error bars correspond to the uncertainties of the spectroscopic method in the region where ZZ Ceti stars are located, $\sigma(T_{\text{eff}}) \sim 200$ K and $\sigma(\log g) \sim 0.05$, as estimated by Fontaine et al. (2003). The dashed lines represent the empirical blue and red edges of the instability strip.

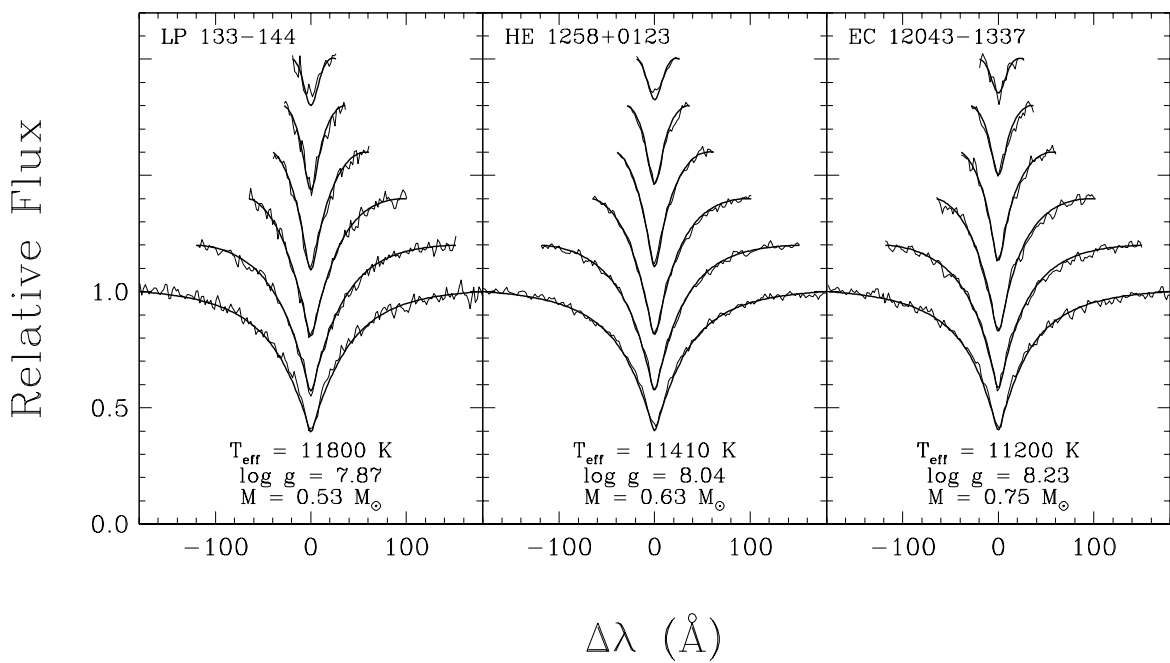


Figure 1

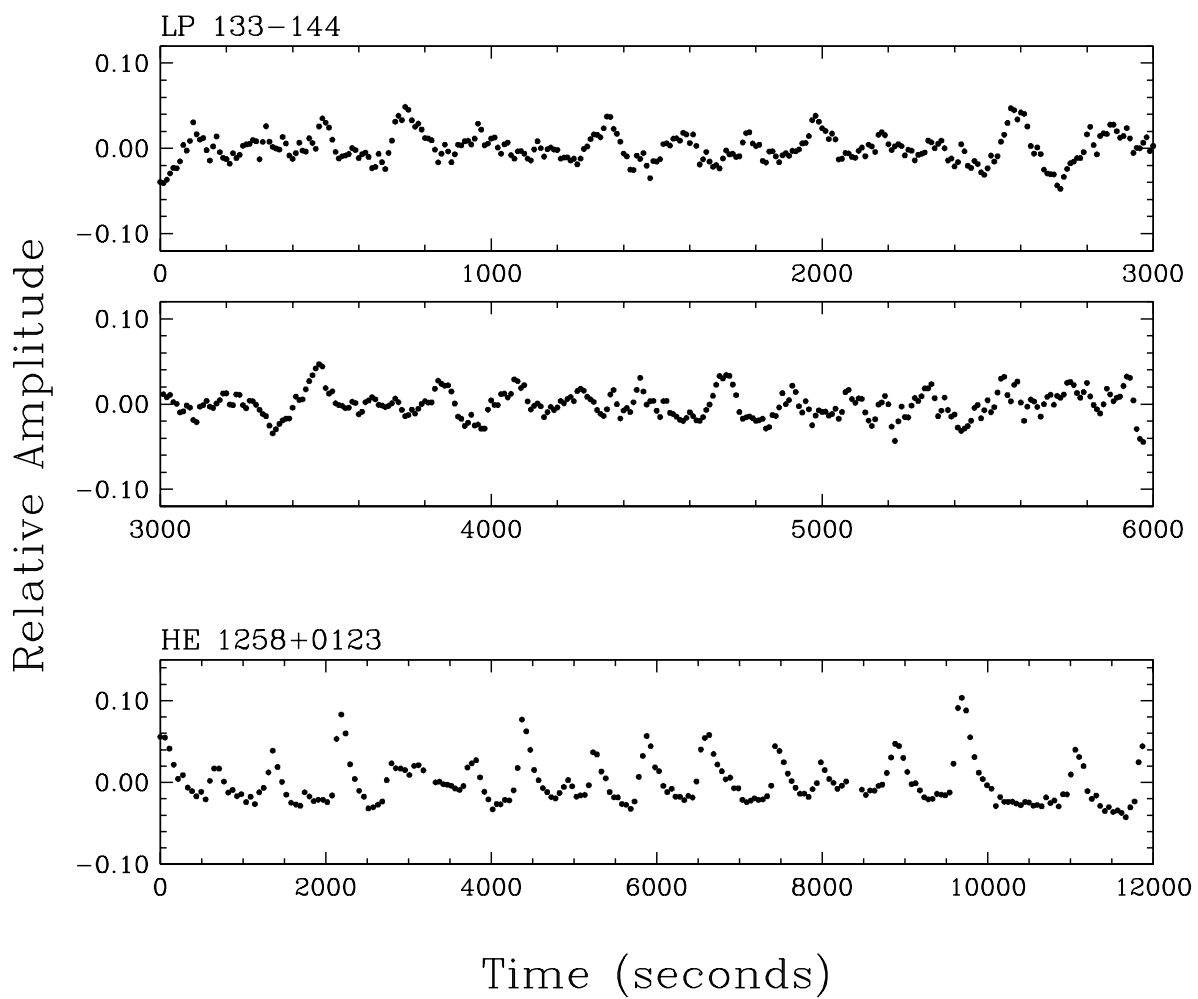


Figure 2

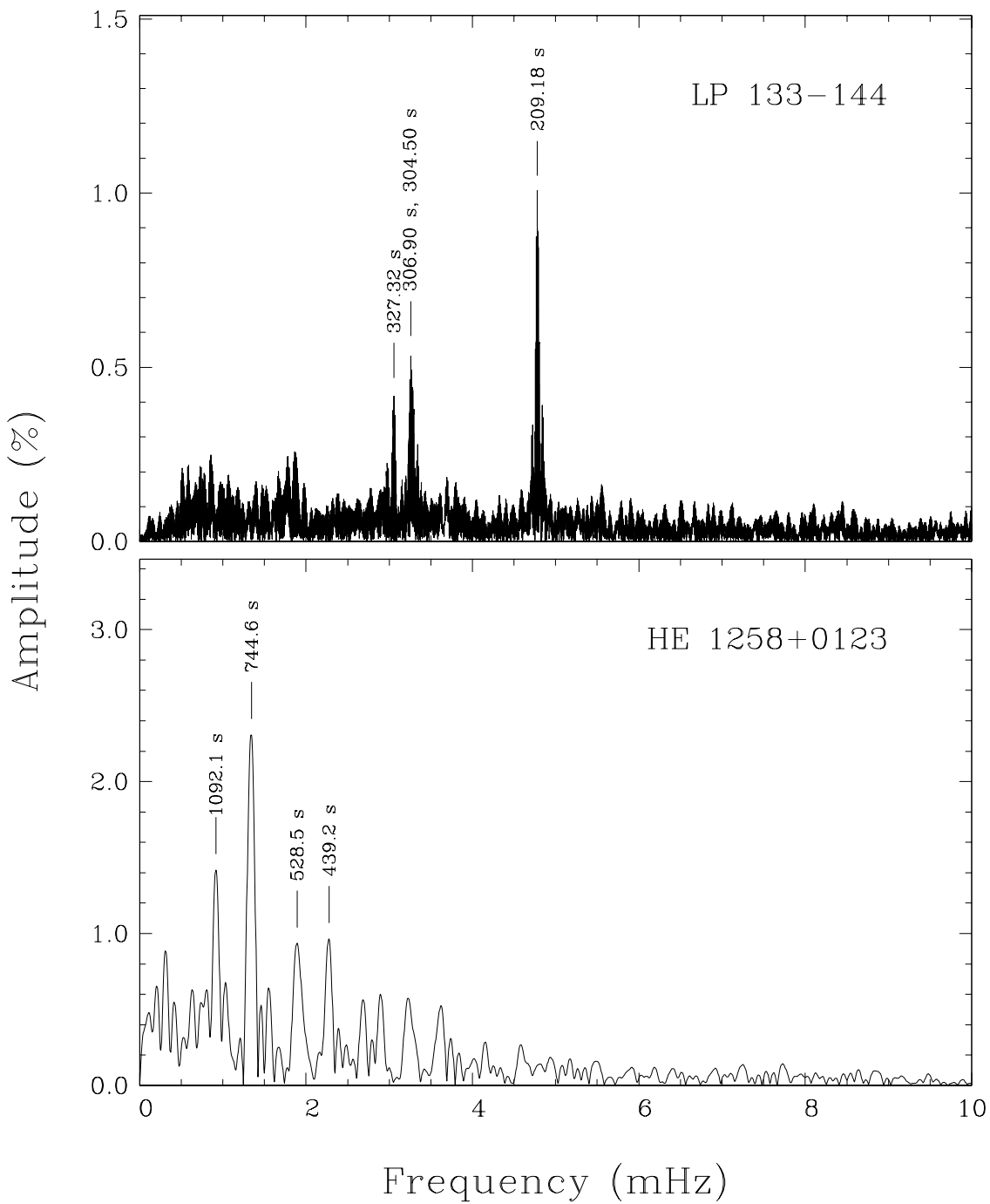


Figure 3

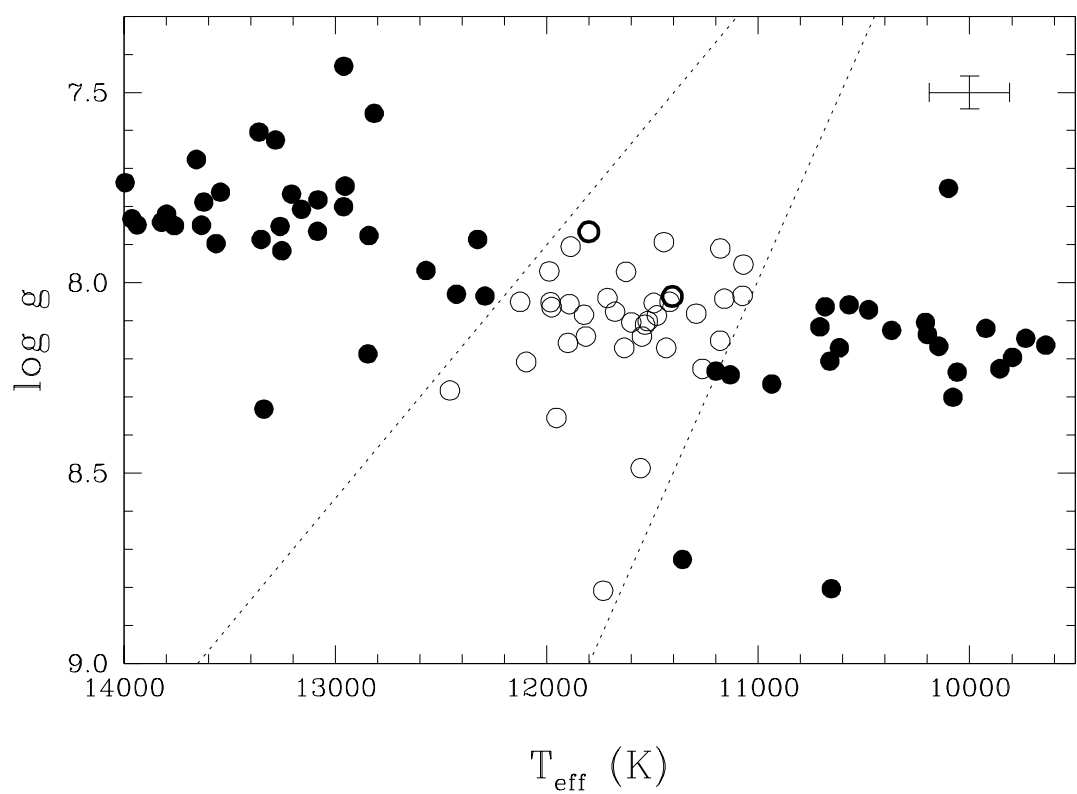


Figure 4